USE OF AN X–RAY PROCESS MODEL TO DETERMINE CRACK DETECTABILITY IN A MULTI-LAYER GEOMETRY

R.M. Wallingford and J.N. Gray
Center for Nondestructive Evaluation and
Center for Aviation Systems Reliability
Iowa State University
Ames, IA 50011

INTRODUCTION

Inspection of a multi-layer geometry is of particular interest to the aircraft industry in which areas repaired with doublers must be continually inspected for further crack growth in the underlying structure. In some muti-layer geometries, x-ray inspection is the modality of choice due to the inaccessibility and limitations of other techniques. Because x-ray inspectability is extremely dependent upon crack opening and orientation, a need exists to quantitatively assess the detectability of cracks for various crack geometry parameters and x-ray generator parameters. X-ray simulation models for different generator types, generator settings, inspection geometries and crack parameters can be used to make these quantitative assessments [1]. The long term goal of this work is to contribute to an inspection standard for certain aircraft geometries which will account for variabilities in generator characteristics such as output spectrum, filtration, voltage and current. In this paper,we target a specific aircraft inspection problem and apply the x-ray simulation model to crack detectability in terms of contrast. In addition, some model validation is performed to support the results of the inspection simulations. Finally, a preliminary quantitative measure of crack detectability in terms of both size and contrast is derived and applied to the simulation results.

INSPECTION PROBLEM

The inspection problem addressed by this work is the rear pressure bulkhead of large commercial aircraft highlighted in Fig. 1. The primary areas of interest are the corners near the doorway through the bulkhead as shown in Fig. 2. These areas consist of multiple layers of aluminum, steel and titanium depending upon the specific location and state of repair. The worst-case material stackup has been selected for analysis and is shown in Fig. 3. In this case, a titanium shim has been used as a doubler for repair over the baseline layers of aluminum and steel. We assume that cracks already exist within the underlying structure (as addressed by the doubler) and we are concerned with further crack growth in interior layers as well as new cracks on the doubler. An increase in the overall stack thickness due to the doubler generally reduces the crack contrast and detectability and a quantitative measure of detectability of cracks in the various layers is desired.

Review of Progress in Quantitative Nondestructive Evaluation, Vol. 12
Edited by D.O. Thompson and D.E. Chimenti, Plenum Press, New York, 1993

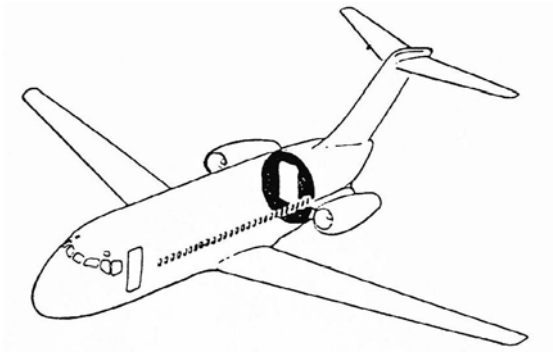

Fig. 1 Aft pressure bulkhead of a large commercial aircraft.

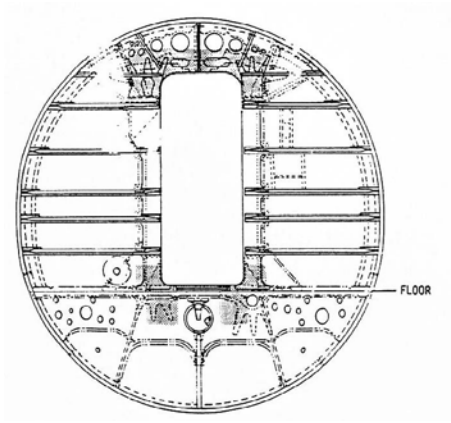

Fig. 2 Areas of interest for the inspection are the corner sections.

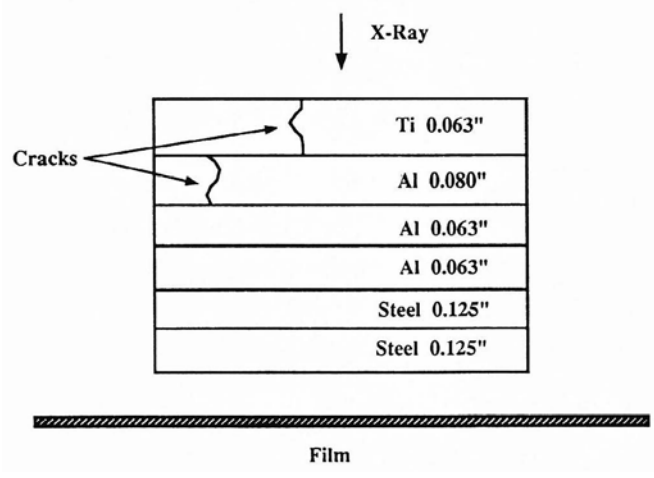

Fig. 3 Worst case stack arrangement for corner inspection.

MODEL VALIDATION

In order to make quantitative predictions of contrast and detectability, the accuracy of the x-ray simulation model must be verified. This verification was done by comparing simulated exposure characteristics and contrast curves with experiment. Exposure characteristics were generated by plotting film density vs. sample thickness at constant generator voltage, and generator voltage vs. sample thickness at a constant film density. These plots were then used to generate contrast curves (contrast vs. sample thickness) at a nominal film density (typically 2.5) for a change in sample thickness of 0.04 inches. The nominal film density of 2.5 was obtained by selecting the voltage required to produce this density at the appropriate sample thickness from the exposure characteristic. Fig. 4 shows comparison plots of the contrast curves for a Sperry SPX-160 generator, a Feinfocus generator and the x-ray simulation model. Error bars on the Feinfocus data were determined through repeated independent experimental trials. Error bars are not included on the Sperry data because they were supplied by an independent organization. Notice that there is fairly good agreement between the model and experiment over at least part of the range of aluminum thickness. One of the sources of discrepancy between the model and experiment is the variation in spectral characteristics of the x-ray generators. The model can be better matched to the Sperry data by modification of the modeled spectrum. This can be accomplished most easily by introducing a filter into the inspection model. Fig. 5 illustrates the change in the contrast curve when a copper filter (0.04") was used in the model. Notice the reduction in contrast at the lower thickness values as well as the good agreement with the Sperry data. The ability to modify the spectral characteristics of the modeled generator is important in accurately predicting contrast and detectability for a specific generator/inspection setup.

INSPECTION SIMULATION

Modeling the inspection of the worst-case stack arrangement shown in Fig. 3 involves predicting contrast data for cracks as a function of crack orientation and generator spectrum. In order to simulate a stack of multiple materials, radiograph equivalence factors must be calculated for the titanium and steel with respect to aluminum. These are computed as a function of generator voltage and are plotted in Fig. 6. Thus, the multiple material stack can be treated as an equivalent aluminum material with a thickness determined by the equivalence factors at the proper generator voltage. The equivalence factors are also used to determine the crack height since we are allowing cracks in the titanium as well as the aluminum, and we are assuming that the cracks break through the entire thickness of an individual layer.

Inspection modeling was performed for 5 mil wide through-cracks in the outer titanium layer and the first aluminum layer using the stack arrangement shown in Fig. 3. The simulation was performed using a 600 mA*sec exposure at a 100 kV generator voltage to yield a background film density of approximately 2.5 using a film model for Kodak M5 radiographic film. The equivalent aluminum thickness for the entire stack at 100 kV is 3.50 inches and the equivalent crack height for a through crack in the titanium layer is 0.30 inches. The crack was modeled as a flattened ellipsoid having principal axis lengths of 0.005 inches, 1.000 inches, and t, where t is the equivalent thickness of the layer containing the crack. The effect of orientation on crack contrast is shown in Fig. 7 for the two cracks. Notice that the crack in the titanium layer has much better contrast at normal incidence due to its larger equivalent height. Also notice that the crack contrast for the aluminum layer decreases very slowly from its value at normal incidence. This indicates that further cracking in underlying layers creates a more difficult inspection problem in terms of flaw contrast.

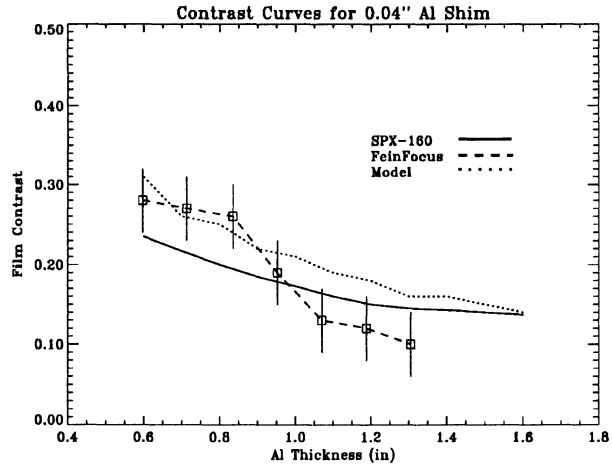

Fig. 4 Comparison of film contrasts for model, SPX-160 and Feinfocus generators.

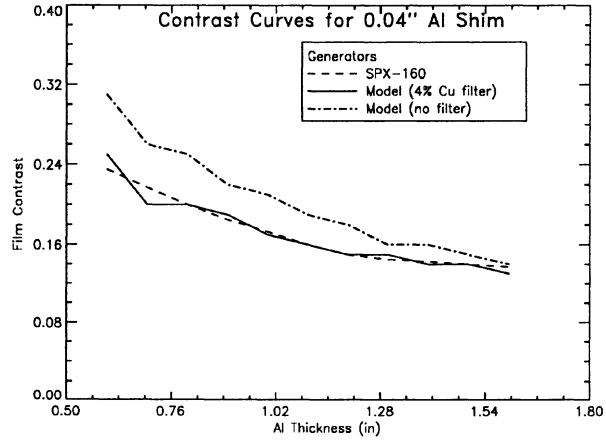

Fig. 5 Comparison of contrast between model and SPX160 (with and without filtration).

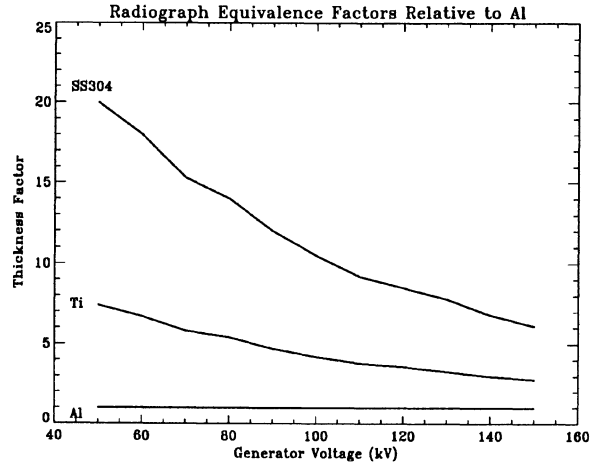

Fig. 6 Radiograph equivalence factors for Ti and SS304 relative to aluminum.

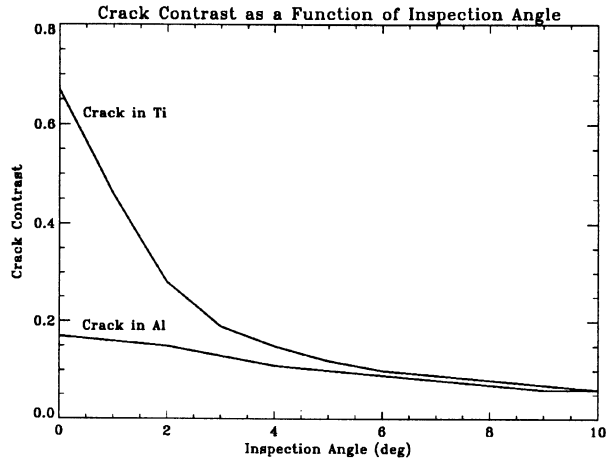

Fig. 7 Crack contrast dependence on angle of inspection

Cracking in the outer titanium layer can also represent a difficult inspection problem if the angle of inspection varies beyond approximately 5 degrees from normal incidence.

X-ray generator output spectrum also plays a role in determining the detectability of cracks. A variation in spectral shape, especially at the low energy region can have a significant effect on flaw contrast and inspection sensitivity. This phenomenon is important in assessing the effects of using different generators (having different output spectra) on crack detectability, especially at critical contrast levels. The x-ray simulation model allows the spectrum to be easily modified by using filters of selectable material and thickness. This type of simulation allows us to quantitatively predict the effect of inherent filtration, and thus, output spectrum on the crack detectability and contrast. Figure 8 illustrates the decrease in sensitivity caused by copper and steel filters added to the simulation of Figure 7. In this case, the simulation used a through-crack in the titanium layer.

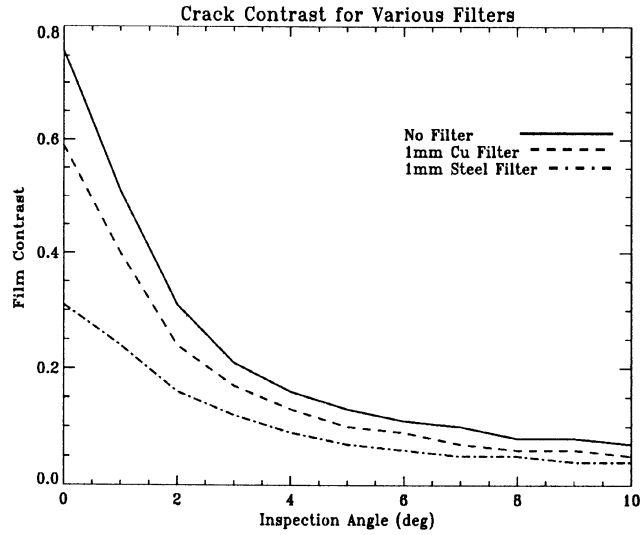

Fig. 8 Illustration of effects of generator filtration on crack contrast.

DETECTABILITY MEASURES

The above analysis yields very useful quantitative information in terms of flaw contrasts and film densities. It doesn't, however, address detectability in the sense that a human viewer is interpreting inspection results and making a decision. One remedy is to assume a minimum detectable contrast and set a critical contrast threshold. This, however, ignores the fact that a critical contrast is dependent on background density. In many inspection situations, the complexity of a part creates wide variations in film density and therefore, the critical contrast depends on the region of interest. In cases where regions on the film are underexposed or overexposed, digital image processing techniques can be used to produce a digitized radiograph having a background density for optimum viewing. In addition, image enhancement techniques can increase critical flaw signals in low contrast, high noise conditions [2,3]. Once the radiograph is digitized,we can apply statistical tests based on the known noise characteristics of the measurement process to determine the statistical significance of potential flaws. In the development of a quantitative detectability measure, we have attempted to link at least part of the formulation to the process in which a human viewer detects contrasts. In particular, flaw area, signal-to-noise ratio, and flaw aspect ratio play important roles in the detection capability of a human viewer [4-6].

We have developed a preliminary method for computing flaw detectability that accounts for flaw area and signal-to-noise ratio and correlates well with human observer performance for some images. The procedure first optimally thresholds a digitized radiograph within regions of stationary data. Consider the image data within a stationary region to be some mathematical combination of a flaw signal and noise. This is a simplifying assumption since we know that radiographic noise consists of signal dependent poisson noise along with colored film grain noise [7,8]. However, we do not need to know the exact mathematical process since we will select the threshold based on a comparison of the candidate region statistics with a region whose statistics are known to be caused by noise alone. Next consider a region within the image having the same average background but known to *not* contain a flaw signal. This can be produced by radiography of a flaw-free material of same thickness under the same conditions. It can also be easily simulated with the x-ray simulation model. We estimate the probability density functions of the candidate region and flaw-free region, p_{n+s} and p_n, by their respective normalized histograms as illustrated in Fig. 9. The optimal threshold is selected by maximizing

$$Q = \sum_{g=t}^{M} p_{s+n}(g) - \sum_{g=t}^{M} p_n(g) \tag{1}$$

over all possible gray levels, g, where M is the maximum gray scale value and t is the threshold. This maximization can be thought of as minimizing the number of noise pixels above the threshold while, at the same time, maximizing the number of signal pixels above the threshold.

We now form a hypothesis that the distribution of thresholded pixels within the image window belongs to the noise distribution, $p_n(g)$. Thus, if we accept the hypothesis, we assume no flaw is present, while if we reject the hypothesis, we assume a flaw is present. Under the assumption of the above hypothesis, each thresholding operation on each pixel within the image window is a Bernoulli trial with a probability of success defined by

$$p_w = \sum_{g=t}^{M} p_n(g) . \tag{2}$$

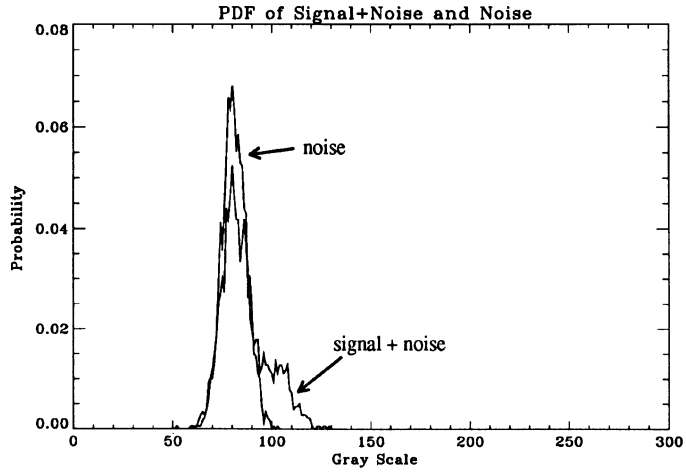

Fig. 9 Probability density functions for signal+noise and noise.

If we consider all of the thresholding operations within the window together, the resulting number of thresholded pixels is governed by the binomial distribution and is given by

$$P(n_w) = \binom{A}{n_w} p_w^{n_w} (1 - p_w)^{A - n_w} \quad . \tag{3}$$

where n_w is the number of thresholded pixels and A is the total number of pixels. The hypothesis test can now be stated as

$$H_o : \frac{n_w}{A} = p_w \qquad H_A : \frac{n_w}{A} > p_w \qquad \alpha$$

where α is the probability of incorrectly rejecting H_o (probability of a type I error). For a large sample, we can approximate the above binomial distribution by a normal distribution having mean, p_w, and variance, $p_w(1-p_w)/A$, which yields the following test statistic [9].

$$z_T = \frac{\frac{n_w}{A} - p_w}{\sqrt{p_w(1-p_w)/A}} \quad . \tag{4}$$

The computed value of z_T is compared against z_α (z-variate having α exceedence probability) and the decision rule is

Accept H_o if $z_T <= z_\alpha$ (no flaw)
Reject H_o if $z_T > z_\alpha$. (flaw)

The above procedure yields the following results when applied to simulated crack images of 0 degree orientation in titanium, 2 degree orientation in aluminum, and 4 degree orientation in aluminum:

Crack	n_w/A	p_w	z_T	$z_{0.01}$	decision
0 degree Ti	0.25	0.05	9.2	2.3	detected
2 degree Al	0.30	0.20	2.5	2.3	detected
4 degree Al	0.25	0.20	1.3	2.3	not detected

These results agree with subjective visual performance when viewing the digitized images on a video display. It should be mentioned that this technique is sensitive to the relative sizes of the flaw area and window area. For very large windowed areas, some small flaws will not create enough bias in p_{n+s} for a reliable detection, even if the contrast is very large. For this reason, a good rule of thumb is to select a window size of similar size to the expected flaw size.

CONCLUSIONS

An x-ray simulation inspection model has been applied to the quantitative study of crack contrast and detectability in a multi-layer, multi-material geometry. This study has been useful in demonstrating the quantitative effects of the contrast on crack orientation, inspection orientation and generator characteristics. We have shown a layer dependence on crack contrast as well as crack angle and generator filtration. This type of analysis has the potential for use in x-ray generator qualification for specific x-ray generator properties and inspection geometries. We have also developed a preliminary detectability measure which shows promise for use where image processing or image enhancement is used for radiographic viewing. Future efforts in these areas will involve further experimental corroboration with the simulation model, especially in the areas of orientation dependence in underlying layers, as well as further refinements of the detectability model.

ACKNOWLEDGMENT

The authors would like to thank Don Hagemaier for his useful advice and discussions related to this work. This work was supported by the Center for Nondestructive Evaluation and the Center for Aviation Systems Reliability at Iowa State University, Ames, IA.

REFERENCES

1. J.N. Gray, F. Inanc and B.E. Shull, "Three Dimensional Modeling of Projection Radiography " in Review of Progress in Quantitative Nondestructive Evaluation, Vol. 8A, D.O. Thompson and D.E. Chimenti, Ed., Plenum Press, 1989.
2. Fundamentals of Digital Image Processing, Anil K. Jain, Prentice Hall, 1989.
3. R.M. Wallingford, E.M. Siwek and J.N. Gray, "Application of Two-dimensional Matched Filters to X-ray Radiographic Flaw Detection" in Review of Progress in Quantitative Nondestructive Evaluation, Vol. 11A, D.O. Thompson and D.E. Chimenti, Ed., Plenum Press, 879-886, 1989.
4. R.G. Swensson and P.F. Judy, "Detection of Noisy Visual Targets: Models for the effects of spatial uncertainty and Signal-to-Noise Ratio" Perception and Psychophysics, Vol. 29, No. 6, 521-534, 1981.
5. P.R. Moran, "A Physical Statistics Theory for Detectability of Target Signals in Noisy Images - Mathematical Background, Empirical Review, and Development of Theory" Medical Physics, Vol. 9, No. 3, 401-413, 1982.
6. M. Ishida, K. Doi, L-N. Loo, C.E. Metz, and J.L. Lehr, "Digital Image Processing: Effect on Detectability of Simulated Low-Contrast Radiographic Patterns" Radiology, Vol. 150, No. 2, 569-575, 1984.
7. Medical Imaging Systems, Albert Macovski, Prentice Hall, 1983.
8. D.T. Kuan, A.A. Sawchuk, T.C. Strand and P. Chavel, "Adaptive Noise Smoothing Filter for Images with Signal-Dependent Noise" IEEE Transactions on Pattern Analysis and Machine Intelligence, Vol. 7, No. 2, 165-177, 1985.
9. A Handbook of Introductory Statistical Methods, C.P. Cox, Wiley, 1987.